AEDC-TDR-63-102

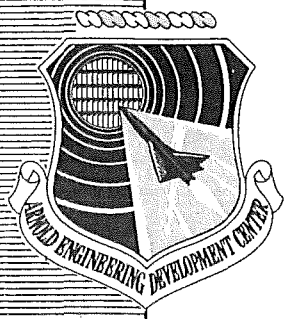

A STUDY OF LAMINAR HEAT TRANSFER TO SPHERICALLY BLUNTED CONES AND HEMISPHERE-CYLINDERS AT HYPERSONIC CONDITIONS

By

B. J. Griffith and Clark H. Lewis
von Kármán Gas Dynamics Facility
ARO, Inc.

TECHNICAL DOCUMENTARY REPORT NO. AEDC-TDR-63-102

June 1963

AFSC Program Area 806A , Project 8951 , Task 895103

(Prepared under Contract No. AF 40(600)-1000 by ARO, Inc., contract operator of AEDC, Arnold Air Force Station, Tenn.)

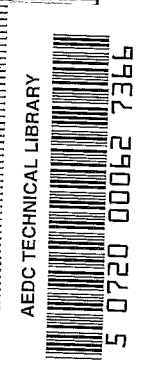

ARNOLD ENGINEERING DEVELOPMENT CENTER
AIR FORCE SYSTEMS COMMAND
UNITED STATES AIR FORCE

NOTICES

Qualified requesters may obtain copies of this report from ASTIA. Orders will be expedited if placed through the librarian or other staff member designated to request and receive documents from ASTIA.

When Government drawings, specifications or other data are used for any purpose other than in connection with a definitely related Government procurement operation, the United States Government thereby incurs no responsibility nor any obligation whatsoever; and the fact that the Government may have formulated, furnished, or in any way supplied the said drawings, specifications, or other data, is not to be regarded by implication or otherwise as in any manner licensing the holder or any other person or corporation, or conveying any rights or permission to manufacture, use, or sell any patented invention that may in any way be related thereto.

A STUDY OF LAMINAR HEAT TRANSFER TO SPHERICALLY BLUNTED CONES AND HEMISPHERE-CYLINDERS AT HYPERSONIC CONDITIONS

By

B. J. Griffith and Clark H. Lewis

von Kármán Gas Dynamics Facility

ARO, Inc.

a subsidiary of Sverdrup and Parcel, Inc.

June 1963

ARO Project No. VT2149

FOREWORD

The study on which this report is based constitutes a part of a research program on viscous effects in hypersonic flow. The research program is sponsored by the U. S. Air Force under Contract AF 40(600)-1000, Project VT2149.

The authors wish to acknowledge the assistance of Mr. E. Burgess of the Scientific Computing Services, ARO, Inc., in providing the computing machine solution and Mr. K. Bird and his staff of Cornell Aeronautical Laboratory for their data.

ABSTRACT

Heat-transfer distribution data obtained in the arc-driven tunnels (hotshot type) of the von Kármán Gas Dynamics Facility, AEDC, are presented. Data were taken on a 9-deg half-angle spherically blunted cone and a hemisphere-cylinder at Mach numbers between 17 and 20 and Reynolds numbers per foot in the free-stream between 100,000 and 800,000.

The test data are compared with theory and available shock tube and shock tunnel results. Good agreement between Lees' theory and measured heat-transfer rates demonstrates the capability of the VKF hotshot tunnels to obtain heat-transfer distribution data. The data indicate a strong dependence of the heat-transfer distribution on pressure distribution, Mach number, and cone half-angle. The heat-transfer data are correlated over a wide range of Mach numbers and cone angles. Correlation curves and formulas are presented for the pressure and heat-transfer distribution to spherically blunted cones at hypersonic conditions.

PUBLICATION REVIEW

This report has been reviewed and publication is approved.

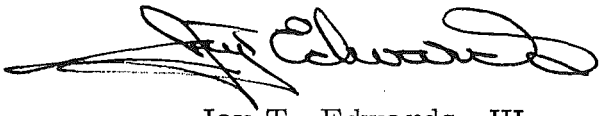

Jay T. Edwards, III
Capt, USAF
Gas Dynamics Division
DCS/Research

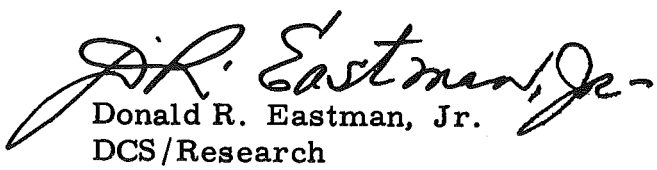

Donald R. Eastman, Jr.
DCS/Research

CONTENTS

ILLUSTRATIONS

NOMENCLATURE

C	Correlation constant (Eq. (5))
C^*	Form of Chapman-Rubesin viscosity coefficient, $\mu_*/\mu_\infty = C_* T_*/T_\infty$
C_H	Heat-transfer coefficient, $\dfrac{\dot{q}_w}{\rho_\infty U_\infty (h_o - h_w)}$
C_p	Pressure coefficient, $\dfrac{p_w - p_\infty}{q_\infty}$
c_p	Specific heat at constant pressure
D_B	Base diameter, in.
d	Nose diameter, in.
g	$C_p/2\theta_c^2$
h	Enthalpy of gas, ft^2/sec^2
h_r	Wilson's reference enthalpy (Eq. (8))
K	Constant in Fay-Riddell equation (Eq. (2))
k	Nose drag coefficient (0.964 for spherically blunted cone)
L	Model length, in.
M	Mach number
p	Pressure
Pr	Prandtl number
q_∞	Dynamic pressure
$\dot{q}$	Heat-transfer rate, Btu/ft^2sec
$\dot{q}_o$	Stagnation heat-transfer rate behind a normal shock
$\dot{q}_{o_w}$	Inferred stagnation heat rate, $\dot{q}_w/(\dot{q}/\dot{q}_o)_{Lees'}$ ($\dot{q}/\dot{q}_o = 0.0465$ for a hemisphere-cylinder at $S/R_o = 2.32$, $M_\infty \sim 18$)
R	Radius, in.
R_B	Base radius, in.
R_o	Nose radius, in.
Re	Free-stream Reynolds number
$Re_\infty/in.$	Free-stream Reynolds number per inch

$Re_{\infty d}$	Free-stream Reynolds number based on nose diameter
S	Entropy
s	Surface distance from stagnation point of model, in.
T	Temperature, °K
T_*	Reference temperature, $(T_o/6)(1 + 3T_w/T_o)$, Ref. 9
t	Time
U	Velocity, ft/sec
W_1, W_2	Parameters defined in Eq. (8)
X	Cheng's axial distance parameter, $(x/d)\theta_c^2/(\epsilon k)^{1/2}$
x	Axial distance, in.
Y	Cheng's modified heat-transfer parameter, see Eq. (3)
Z	Compressibility factor
γ	Ratio of specific heats, c_p/c_v
ϵ	$(\gamma-1)/\gamma+1$
θ_c	Cone half-angle, radians unless otherwise noted
μ	Gas viscosity
ξ	s/R_o
ρ	Density, slugs/ft^3
ψ	Nose bluntness ratio, R_o/R_B

SUBSCRIPTS

AC	Based on computed average conditions in arc-chamber
a	Conditions at one atmosphere pressure and 273.16°K
adw	Adiabatic wall conditions
BW	Blast-wave velocity (measured)
e	Local conditions at the edge of the boundary layer
i	Initial conditions
o	Free-stream stagnation conditions
o'	Stagnation conditions behind a normal shock

$\dot{q}_o$	Based on measured stagnation heat rate
$\dot{q}_{o_w}$	Based on inferred stagnation heat rate
r	Condition at reference enthalpy, h_r
w	Wall conditions
∞	Free-stream conditions
*	Conditions at reference temperature, T_*

1.0 INTRODUCTION

The capability of the hypervelocity (hotshot-type) tunnels of the von Kármán Gas Dynamics Facility (VKF), Arnold Engineering Development Center (AEDC), Air Force Systems Command (AFSC), to obtain pressure distribution and force data has been demonstrated in a series of recent reports (Refs. 1 through 5). The purpose of the present report is to demonstrate a similar capability to obtain heat-transfer data in nitrogen at Mach numbers between 17 and 20 and Reynolds numbers per foot between 100,000 and 800,000. Data are presented from the three hypervelocity tunnels of the VKF: (1) 16-in. (Hotshot 1), (2) 50-in. (Hotshot 2), and (3) 100-in. (Tunnel F).

The tests reported herein were conducted on spherically blunted cones and hemisphere-cylinders. The results are compared with data from Cornell Aeronautical Laboratory's (CAL) shock tunnels on flat-nosed slender cones (Ref. 6) and spherically blunted cones (Ref. 7)*.

The experimental results are compared with the theoretical prediction of heat-transfer distribution by Lees (Ref. 8), Cheng (Ref. 9), and the conical flow sharp cone value. Theoretical heat-transfer curves are presented for a wide range of Mach numbers and cone half-angles.

Correlations are presented based upon a modification of Cheng's heat-transfer parameter. A simple correlation of the heat-transfer distribution over blunted cones which is adequate for engineering estimates is also given.

2.0 TEST DESCRIPTION

2.1 TUNNEL AND TEST CONDITIONS

Detailed descriptions of the three AEDC-VKF hypervelocity (hotshot) tunnels are given in Refs. 1, 2, 10, and 11. The conditions for the tests in these tunnels are shown on the following page.

---

*AEDC sponsored research

Manuscript received April 1963.

Test Section Diam	M_∞	p_O, psia	T_O, °K	Re_∞/in. x 10^{-3}	Model
100-in. (Tunnel F)	≈20	7400-7700	3300-4000	8-11	9-deg Cone
50-in. (Hotshot 2)	~19	6000-7000	2800-3700	9-15	9-deg Cone
16-in. (Hotshot 1)	17-19	12,000-15,000	2500-4000	25-70	Hemisphere-Cylinder

2.2 MODEL INSTRUMENTATION

The 9-deg half-angle cone (Fig. 2) was fabricated of type 303 nonmagnetic stainless steel. The cone model was instrumented with VKF heat-transfer gages and pressure transducers. Insulation of the model from the tunnel support system was achieved by a nylon sleeve over the model's sting. The hemisphere-cylinder was constructed and instrumented similarly to the spherically blunted cone.

The heat-transfer gage consists of a copper disc held in place by a thermally insulating material with a thermocouple soldered to the back face to sense the disc temperature. A detailed description of the gage is given in Ref. 12. The stagnation point gage was 0.020-in. thick, whereas the other gages were 0.003-in. thick.

Figure 3 shows a typical installation of a thermocouple gage. Calibration of the thermocouple gages with a torch flame and standard calorimeter was within ±10 percent of the theoretical calibration factors based on disc mass, specific heat, and thermocouple output.

3.0 PRECISION

3.1 FLOW CONDITIONS

Until recently, flow conditions were determined as described in Ref. 16. This method is summarized as follows:

Measure initial pressure and density in arc-chamber, p_{O_i} and ρ_{O_i}.

Calculate initial enthalpy, entropy, and temperature, h_{O_i}, S_{O_i}, and T_{O_i}.

Measure timewise decay of pressure in arc-chamber, dp_O/dt.

Calculate timewise decay of density in arc-chamber.

Calculate timewise decay of enthalpy, entropy, and temperature.

Measure instantaneous pitot pressure in test section, $p_{o'}$.

Calculate instantaneous values of flow conditions in test section (M, Re, etc.) based on instantaneous values of ρ_o, p_o, T_o, h_o, S_o, and $p_{o'}$, assuming isentropic expansion from arc-chamber to test section.

Complete space uniformity of gas properties in arc-chamber (T_o, ρ_o, p_o) are necessarily assumed in this method.

Experiments in which instantaneous flow velocity was measured from the translation of blast waves through the test section showed that velocity calculated as described above frequently differed radically from the measured velocity. These experiments also showed that velocity calculated from measured heat-transfer rates was in good agreement with the measured blast-wave velocity. These experiments are described in Ref. 2, and results are summarized in Fig. 4a. Referring to Fig. 4a, it is seen that velocity determined from stagnation point heat-transfer rates measured at the nose of a hemisphere-cylinder ($\dot{q}_o$) or inferred from heat-transfer rates measured beyond the shoulder of the hemisphere ($\dot{q}_{o_W}$) agreed with the measured blast-wave velocity within ±5 percent.

Figure 4b presents typical timewise velocity data. Note that the agreement between the velocity measurements $U_{\dot{q}_o}$ and U_{BW} is excellent even when the velocity U_{AC} is radically different. Clearly the earlier method frequently yielded erroneous flow conditions.

A revised method for determining flow conditions has been adopted and is used in this report. Briefly this method is summarized as follows:

Instantaneous values of p_o and $p_{o'}$ are measured.

Instantaneous values of $\dot{q}_o$ are either measured directly or inferred from a measurement of $\dot{q}_W$ using Lees' distribution theory with experimental pressure distribution, Ref. 8.

Velocity, hence enthalpy (h_o), is calculated from measured values of $p_{o'}$, $\dot{q}_o$, and the heat probe radius, using Fay-Riddell theory, Ref. 13; Newtonian pressure distribution near the stagnation point and zero dissociation are assumed.

With values of p_o, $p_{o'}$, and h_o known, the remaining flow conditions (M, Re, etc.) are calculated as described in Ref. 16.

Use of this revised method has improved greatly the consistency of results for the VKF hotshot tunnels and has simplified calculation of

flow conditions in that the laborious calculation of timewise decay of density in the arc-chamber has been eliminated.

The dual gage heat probe used to measure $\dot{q}_o$ and $\dot{q}_w$ also serves as an excellent contamination monitor. If solid particle contamination is present in the flowing gas, the measured value of $\dot{q}_o$ will be higher than the correct value because of particle impingement at the nose of the probe. The measured value of $\dot{q}_w$ will not be affected by solid particles. Thus, a comparison of the measured $\dot{q}_o$ with a value of $\dot{q}_{ow}$ inferred from the measured value of $\dot{q}_w$ will indicate the presence of, or lack of, particles in the flow. Typically these values agree within ±10 percent, indicating negligible solid particle contamination. Occasionally these measurements indicate a "dirty" run. The frequency of such occasions is small, and data from such runs are not used.

3.2 MEASURED DATA

The precision of the heat-transfer and pressure data obtained in the present investigation was estimated as follows:

Hypervelocity Tunnels	Model	Precision, Percent	
		Pressure	Heat Transfer
16-in. (Hotshot 1)	Hemisphere-Cylinder	±8	±13
50-in. (Hotshot 2)	9-deg Cone	±5	±10
100-in. (Tunnel F)	9-deg Cone	±5	±10

All of the data presented herein were obtained in conical nozzles. Whitfield and Norfleet (Ref. 4) discussed the influence that source flow effects have on pressure measurements over slender sharp cones in conical hypervelocity nozzles. No corrections for possible source flow effects were considered in the results presented herein since they were considered to be negligible.

4.0 THEORETICAL CONSIDERATIONS

4.1 PRESSURE DISTRIBUTIONS

The correlation of pressure distributions in terms of parameters proposed by Cheng (Ref. 9) was used to specify the pressure distributions for the blunted cones considered in this report. The data of Lewis

(Ref. 3) and CAL (Ref. 7) were replotted along with other VKF data in terms of pressure coefficient (Fig. 5). Note that the data of Fig. 5 show no dependence of pressure coefficient on Mach number. Cheng's parameter, $p_W/M_\infty^2\, p_\infty\, \theta_c^2\, \gamma_\infty$ is, of course, equivalent to $C_p/2\theta_c^2$ when $p_W >> p_\infty$. For slender cones at only moderate hypersonic Mach numbers (~ 10), this condition cannot be satisfied; thus the use of $C_p/2\theta_c^2$ is expected to be more general, and the correlation of the available experimental pressure data (Fig. 5) bears out this expectation.

The General Electric Company's real gas characteristics solution (Refs. 3 and 15) and the sharp cone value of Whitfield and Norfleet (Ref. 4) agree well with the experimental data (Fig. 5). All theoretical calculations (except the conical shock values) were made using this characteristics solution and the sharp cone value of Ref. 4, together with an approximate interpolation curve. Shown also in Fig. 5 is the perfect gas, sharp cone (with attached conical shock) value for $M_\infty = 15$ and $\theta_c = 9$ deg.

4.2 HEAT-TRANSFER CALCULATIONS

4.2.1 Blunted Cones

The heat-transfer computations were made using Lees' theoretical distribution (Ref. 8) over the cone surface. The pressure distribution was obtained from Fig. 5 and modified Newtonian over the spherically blunted nose. Local conditions at the edge of the boundary layer (denoted by subscript e) were calculated for an isentropic expansion from the stagnation conditions behind a normal shock (denoted by $()_o'$).

Lees' equation is:

$$\dot{q}_w/\dot{q}_o = \frac{\frac{1}{2}\,\frac{p_w}{p_o'}\,\frac{U_e}{U_\infty}\,\frac{R}{R_o}}{\left[\int_o^\xi \frac{p_w}{p_o'}\,\frac{U_e}{U_\infty}\left(\frac{R}{R_o}\right)^2 d\xi\right]^{1/2}} \left[\frac{U_\infty^2\,\rho_o'}{2(p_o' - p_\infty)}\right]^{1/4} \tag{1}$$

Stagnation point heat-transfer was calculated based upon the Fay-Riddell (Ref. 13) theory for a 300°K wall temperature. The equation used was:

$$\dot{q}_o \sqrt{R_o} = K \left(\frac{\rho_w}{\rho_a}\right)^{0.1} \left(\frac{\rho_o'}{\rho_a}\,\mu_o'\right)^{0.4} (h_o - h_w) \left(\frac{p_o' - p_\infty}{\rho_o'/\rho_a}\right)^{0.25} \tag{2}$$

where

$$K = 1.7044 \times 10^{-3} \text{ for nitrogen}$$

$$= 1.7247 \times 10^{-3} \text{ for air}$$

and the dimensions of $\dot{q}_o \sqrt{R_o}$ are Btu-$\sqrt{\text{in.}}$/ft^{2}sec, and the pressure is in atm.

The heat-transfer calculations were made considering both perfect gas properties and real gas properties from Refs. 14 and 17. All calculations were for stagnation temperatures of 4000°K or less. As noted by Kemp, Rose, and Detra (Ref. 18), the effect of γ on heat-transfer distributions was negligible. The ratio of specific heats (γ) affects the test section parameters during isentropic nozzle flow expansions and thereby would have some influence upon Cheng's correlation parameter. However, for the conditions covered in this paper these effects are only about five percent.

Cheng (Ref. 9), in the development of his theory, assumed p_w/p_o' constant with Mach number and proportional to θ_c^2 for $M_\infty^2 \theta_c^2 >> 1$. Figure 5 indicates that $C_p/2\theta_c^2$ is independent of M_∞ at hypersonic conditions. As noted previously, Cheng's parameter implies that $p_w >> p_\infty$; thus, expressing the heat-transfer data in terms of Cheng's correlation parameter will result in curves (see Fig. 6a) with a Mach number and cone angle dependence and converging at high Mach numbers and larger cone angles. This dependence is caused by the strong influence that p_∞/p_o' has at the lower hypersonic Mach numbers and on the more slender half-angle cones. A modification of Cheng's heat-transfer parameter can be accomplished to account for the fact that p_w is not always much larger than p_∞. Instead of assuming, as Cheng does,

$$p_w/p_o' \propto \theta_c^2$$

use the relation

$$p_w/p_o' = C_p + 2/\gamma M_\infty^2$$

or

$$p_w/p_o' \propto (\theta_c^2 + 1/\gamma g M_\infty^2)$$

where $g \equiv C_p/2\theta_c^2$, which is, as shown in Fig. 5, a unique function of Cheng's distance parameter, $(x/d)\,\theta_c^2/\sqrt{\epsilon k}$. The modified version of Cheng's heat-transfer correlation parameter then becomes

$$Y \equiv \frac{(\epsilon k)^{1/4} C_H \sqrt{Re_{\infty_d}}}{M_\infty (\theta_c^2 + 1/\gamma g M_\infty^2) \sqrt{C_*}} \qquad (3)$$

The theoretical distributions in Fig. 6a are presented in Fig. 6b in terms of this modified correlation parameter. The improvement in using the modified correlation is apparent.

Considering the theoretical heat-transfer distributions for the extreme flow conditions and cone angles encountered here (see Fig. 9) suggests that

$$\dot{q}_w/\dot{q}_o \propto p_w/p_o' \tag{4}$$

Expressing p_w/p_o' in terms of C_p, one obtains

$$\dot{q}_w/\dot{q}_o = C(q_\infty/p_o')\left[C_p + 2/\gamma M_\infty^2\right] \tag{5}$$

where C is a correlation constant to be determined from the previously discussed theoretical solutions. From the perfect gas ($\gamma = 1.4$) solutions, $C = 1.47$ and $q_\infty/p_o' = 0.5436$ for $M_\infty \rightarrow \infty$. The final result is

$$\dot{q}_w/\dot{q}_o = 0.80\ (C_p + 2/\gamma M_\infty^2) \tag{6}$$

for values of $(x/d)\ \theta_c^2/\sqrt{\epsilon k}$ between 0.05 to 0.60.

The heat-transfer distribution over the hemisphere-cylinder was computed in a completely similar manner to the blunt cone calculations. The experimental pressure distributions of Fig. 11 were used as input data to the Lees' equation.

4.2.2 Sharp Cones

Soloman (Ref. 23) gives the following formula for the heat-transfer rate to a sharp cone (with attached conical shock) in an equilibrium real gas:

$$\dot{q}_w = 0.575\ Pr^{-2/3}\ (h_{adw} - h_w)\ \sqrt{\rho_r\ \mu_r\ U_e/s} \tag{7}$$

where $\rho_r\mu_r$ is evaluated at the Wilson (Ref. 24) reference enthalpy

$$h_r = 0.9\ W_1\ (h_w + h_e) + 1.08\ W_2\ (U_e^2/2) + h_e\ (1 - 1.8\ W_1) \tag{8}$$

where

$$W_1 \equiv 1 - 1/2\ (Pr_r)^{1/4}$$

$$W_2 \equiv \left[(Pr_r)^{1/4}/2 - (Pr_r)^{1/3}/3\right]\ (Pr_r)^{1/2}$$

Substituting Eq. (7) into the modified Cheng correlation parameter, Eq. (3), yields

$$Y = 0.575\ Pr^{-2/3}\ \sqrt{\frac{\rho_r\,\mu_r}{\rho_\infty\,\mu_\infty}\ \frac{U_c}{U_\infty}\ \frac{\cos\theta_c}{X}}\ \theta_c\left\{M_\infty\ \sqrt{C_*}\left[\theta_c^2 + (\gamma M_\infty^2 g)^{-1}\right]\right\}^{-1} \tag{9}$$

where

$$X \equiv (x/d)\ \theta_c^2 / \sqrt{\epsilon k}$$

For the conditions considered here (perfect gas, 5 deg $\leq \theta_c \leq$ 15 deg, $10 \leq M_\infty \leq 20$), it was found that $h_r = c_p T_*$ within a percent or so. A comparison of the definition of Cheng's T_* (Ref. 9) with Wilson's T_r (Ref. 24) clearly indicates this. Thus, for $Pr_r = 0.71$ (constant), Eq. (9) becomes

$$Y\sqrt{X} = 0.7224 \sqrt{\frac{U_e}{U_\infty} \frac{\cos \theta_c}{p_w / p_\infty}} \left(\frac{p_w}{p_\infty} - 1 \right) \Bigg/ M_\infty \theta_c \qquad (10)$$

One thus sees that $Y = Y(X^{-1/2};\ M_\infty,\ \theta_c)$ for a sharp cone and is, of course, now independent of the nose diameter.

5.0 RESULTS AND DISCUSSION

5.1 CONES

The experimental heat-transfer rates shown in Figs. 7 and 8 are compared with the theory of Lees' (Ref. 8) and Cheng (Ref. 9). Experimental points include data from the VKF tunnels, data of Wittliff and Wilson (Ref. 6) for a 5-deg half-angle flat-nose cone, and CAL data from Ref. 7.

Figure 7 presents data on slender cones with spherically blunted noses in terms of the modified Cheng parameter. Note the agreement between the test data and Lees' theory for cones with a wide range of nose bluntness ratios. The theoretical computation of Lees' theory in Fig. 7 includes real gas effects; however, as previously noted, within the flow region covered by this paper the real gas effects change the theoretical calculations by only about five percent.

The good agreement between Lees' theory and the sharper 6.34- and 9-deg cones must be considered, at present, fortuitous. Certainly, the normal shock approximation used in calculating the local flow properties over the cone should be invalid for the sharper cones. However, Whitfield and Griffith (Ref. 25) reported similarly good agreement between theoretical estimates (normal shock theory) and experimental cold-wall zero-lift drag data from sharp cones. Figure 7 also presents a theoretical solution for a conical shock case ($M_\infty = 15$, $\theta_c = 9$ deg). This case simply assumes that the cone surface pressure is constant at its inviscid value. Solutions for other Mach numbers and cone

half-angles obtained (but not shown here) fell within ±10 percent of the theoretical sharp cone value shown.

Comparison of the flat-nosed cone data of Ref. 6 with Lees' theory is shown in Fig. 8. The data have been corrected to correspond to the definition of the reference temperature (T_*) used herein. The constant 3 was inadvertently dropped in the original machine data reduction (Ref. 19); this amounts to about a 4-percent correction. In the calculation of the theory, a spherically blunted nose was assumed.

The theoretical heat-transfer distributions have been correlated (see Fig. 9) as a function of p_w/p_o'. Figure 9 shows a comparison between the experimental data for the 6.34- and 9-deg blunt cones of Fig. 7 and Eq. (6). The correlation equation (Eq. (6)) represents a good engineering approximation for the heat-transfer distribution over the afterbodies of spherically blunted cones at hypersonic speeds. The correlation was tested for $0.05 < \left[\theta_c^2/(\epsilon k)^{1/2}\right](x/d) \leq 0.6$.

The 50-in. and 100-in. tunnel heat-transfer data are also presented in the form of ratios of measured surface rates to the stagnation rate (Fig. 10). This facilitates further use of the data and is also convenient for comparison directly with Lees' theory. The measured heat-transfer rate distribution is compared to Lees' theory and data from CAL on a similar model. Note the excellent agreement between Lees' theory and the VKF and CAL data. Lees' theory was calculated using the pressure correlation curve shown in Fig. 5. The VKF and CAL experimental pressure distribution data on the 9-deg blunt cones are also shown in Fig. 10 and substantiate the use of the characteristics solution for the pressure correlation.

5.2 HEMISPHERE-CYLINDERS

Measurements of pressure distribution by Baer (Ref. 20) in the VKF 50-in. hypersonic tunnel at $M_\infty = 8.1$, Kubota (Ref. 21) at $M_\infty = 7.7$, Kemp, et al. (Ref. 18), and by Boison (Ref. 22) in the 16-in. hotshot tunnel, as well as recent measurements in nitrogen in Hotshot 1, are shown in Fig. 11. Note the Mach number dependence of the pressure distribution over a hemisphere-cylinder.

The measured heat-transfer distribution over a hemisphere-cylinder is shown in Fig. 12. Shown also are data from Kemp, Rose, and Detra (Ref. 18) at $M_\infty \approx 2.1$ in the AVCO shock tube. As previously noted by these investigators, the heat-transfer distribution is in general agreement with Lees' theory over the hemispherical nose based upon their measured pressure distribution. Previously unreported measurements at $M_\infty = 8.15$ in the VKF 50-in. hypersonic tunnel are also shown for comparison.

The agreement between heat-transfer measurements in the hotshot tunnels and Lees' theory is notable. The theory is based upon the assumption that the pressure gradient term in the momentum equation is negligible (see Ref. 8). Hence, one might expect the theory to break down for large (favorable) pressure gradients such as in the hotshot tunnels. However, even under conditions of rather strong pressure gradient the agreement between theory and experiment remains good.

The strong dependence of heat transfer on pressure distribution is clearly shown by the AVCO and hotshot tunnel results. It is therefore not satisfactory to use shock tube results for $M_\infty \approx 2$ to predict heat-transfer distributions over blunt bodies at hypervelocity conditions.

6.0 CONCLUSIONS

Based on this investigation to demonstrate the capability to obtain heat-transfer data in nitrogen at Mach numbers 17 and 20 and Reynolds numbers per foot between 100,000 and 800,000 in the AEDC hypervelocity tunnels, the following conclusions are made:

1. The agreement between the heat-transfer data on a 9-deg blunt cone and a hemisphere-cylinder with Lees' theory and other available data demonstrates the capability of conducting heat-transfer tests on hypersonic vehicles in the VKF hotshot tunnels.
2. The pressure distribution correlation is independent of Mach number and cone angle when expressed in terms of a modification of the parameters proposed by Cheng (Ref. 9).
3. The heat-transfer distribution is independent of Mach number and cone angle when expressed in terms of a modification of the heat-transfer parameters proposed by Cheng (Ref. 9).
4. The strong dependence of heat transfer on pressure distribution clearly suggests that it is not satisfactory to use the shock tube results for $M_\infty \approx 2$ to predict heat-transfer distributions over blunt bodies at hypervelocity conditions.
5. A good engineering approximation for the heat-transfer distribution over blunted cones for $\left[\theta_c{}^2/(\epsilon k)^{1/2}\right] x/d$ between 0.05 and 0.6 is $\dot{q}_w/\dot{q}_o = 0.80\ (C_p + 2/\gamma M_\infty{}^2)$.

REFERENCES

1. Lukasiewicz, J., Whitfield, J. D., and Jackson, R. "Aerodynamic Testing at Mach Numbers from 15 to 20." Hypersonic Flow Research, Progress in Astronautics and Rocketry, 7, Academic Press, 1962, 473-511 (Paper presented at ARS Symposium, Hypersonics Conference held at MIT, August 1961.)

2. Lukasiewicz, J., Jackson, R., and Whitfield, J. D. "Status of Development of Hotshot Tunnels at the AEDC." (Paper given at AGARD Meeting, Rhode-Saint-Genese, Belgium, April 1962.) Preprint available from AEDC.

3. Lewis, C. H. "Pressure Distribution and Shock Shape over Blunted Slender Cones at Mach Numbers from 16 to 19." AEDC-TN-61-81, August 1961.

4. Whitfield, J. D. and Norfleet, G. D. "Source Flow Effects in Conical Hypervelocity Nozzles." AEDC-TDR-62-116, May 1962.

5. Whitfield, J. D. and Wolny, W. "Hypersonic Static Stability of Blunt Slender Cones." AEDC-TDR-62-166, August 1962.

6. Whittliff, C. E. and Wilson, M. R. (a) "An Investigation of Laminar Heat Transfer to Slender Cones in the Hypersonic Shock Tunnel," CAL Report AF-1270-A-2 (WADD-TN 59-6), May 1961. Also "Heat Transfer to Slender Cones in Hypersonic Air Flow Including Yaw and Nose-Bluntness Effects," (b) Paper presented at the IAS/ARS Joint Meeting June 1961, Paper No. 61-213-1907, and (c) Journal of the Aero/Space Sciences, Vol. 29, No. 7, July 1962, pp. 761-774.

7. Cornell Aeronautical Laboratory. "Hypersonic Force, Pressure and Heat Transfer Investigations of Sharp and Blunt Slender Cones." (AEDC-TDR to be published.)

8. Lees, Lester, "Laminar Heat Transfer over Blunt-Nosed Bodies at Hypersonic Flight Speeds." Jet Propulsion, Vol. 26, No. 4, April 1956, p. 259.

9. Cheng, H. K. "Hypersonic Flow with Combined Leading-Edge Bluntness and Boundary-Layer Displacement Effect." CAL Report AF-1285-A-4, Nonr 2653(00), August 1960.

10. Lukasiewicz, J., Harris, W. G., Jackson, R., van der Bliek, J.A., and Miller, R. M. "Development of Capacitance and Inductance Driven Hotshot Tunnels." AEDC-TN-60-222, January 1961.

11. van der Bliek, J. A., Deskins, H. E., and Walker, R. R. III. "Further Development of an Inductance-Driven Hotshot Tunnel." AEDC-TN-61-80, July 1961.

12. Ledford, R. L. "A Device for Measuring Heat-Transfer Rates in Arc Discharge Hypervelocity Wind Tunnels." AEDC-TDR-62-64, May 1962.

13. Fay, J. A. and Riddell, F. R. "Theory of Stagnation Point Heat Transfer in Dissociated Air." Journal of Aero/Space Sciences, Vol. 25, No. 2, February 1958, pp. 73-85, 121.

14. Hilsenrath, J. "A First Approximation to the Thermodynamic Properties of Nitrogen." National Bureau of Standards, Preliminary Draft (Unpublished), May 1959.

15. General Electric Company, Private communications from H. Ridyard.

16. Grabau, Martin, Humphrey, Richard L., and Little, Wanda J. "Determination of Test-Section, After-Shock, and Stagnation Conditions in Hotshot Tunnels Using Real Nitrogen at Temperatures from 3000 to 4000°K." AEDC-TN-61-82, July 1961.

17. Landis, F. and Nilson, E. N. "Thermodynamic Properties of Ionized and Dissociated Air from 1500°K to 15,000°K." Pratt and Whitney Aircraft Report No. 1921, January 1961.

18. Kemp, N. H., Rose, P. H., and Detra, R. W. "Laminar Heat Transfer around Blunt Bodies in Dissociated Air." AVCO Research Report 15, May 1958. (Also Journal of the Aero/Space Sciences, Vol. 26, No. 7, July 1959, pp. 421-430).

19. Cornell Aeronautical Laboratory. Private communications from Charles E. Wittliff.

20. Baer, A. L. "Pressure Distributions on a Hemisphere Cylinder at Supersonic and Hypersonic Mach Numbers." AEDC-TN-61-96, August 1961.

21. Kubota, Toshi. "Investigation of Flow around Simple Bodies in Hypersonic Flow." California Institute of Technology Memo No. 40, June 1957.

22. Boison, J. C. "Experimental Investigation of the Hemisphere Cylinder at Hypervelocities in Air." AEDC-TR-58-20, November 1958.

23. Soloman, Jay M. "The Calculation of Laminar Boundary Layers in Equilibrium Dissociated Air by an Extension of the Cohen and Reshotko Method." NOL-TR-61-143, February 1962.

24. Wilson, R. E. "Real Gas Laminar Boundary Layer-Skin Friction and Heat Transfer." Journal of the Aero/Space Sciences, Vol. 29, No. 6, June 1962, pp. 640-647.

25. Whitfield, Jack D. and Griffith, B. J. "Viscous Effects on Zero-Lift Drag of Slender Blunt Cones." AEDC-TDR-63-35, March 1963.

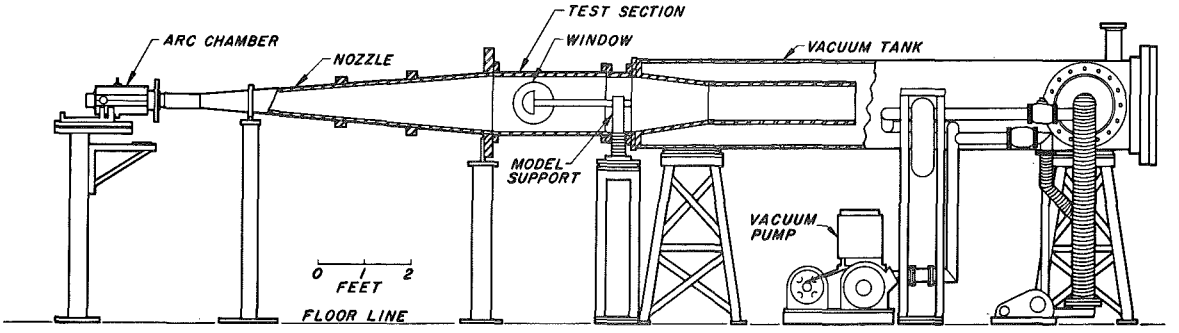

a. 16-Inch Hotshot

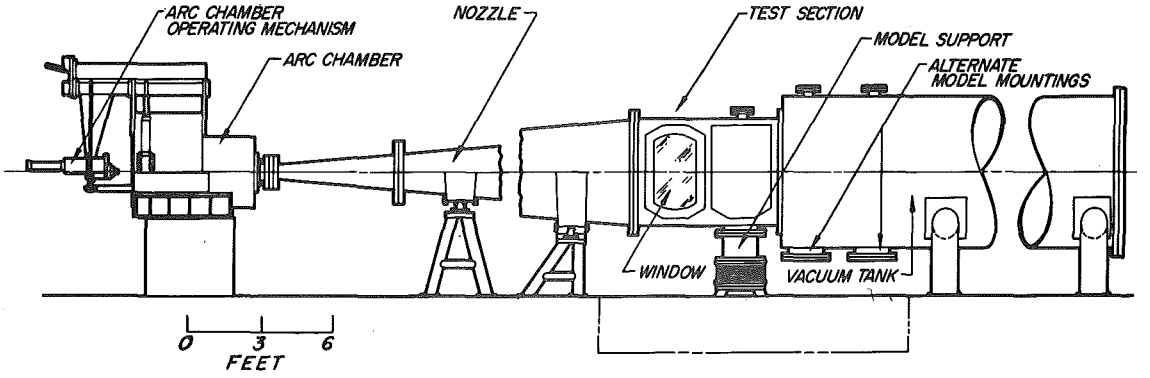

b. 50-Inch Hotshot

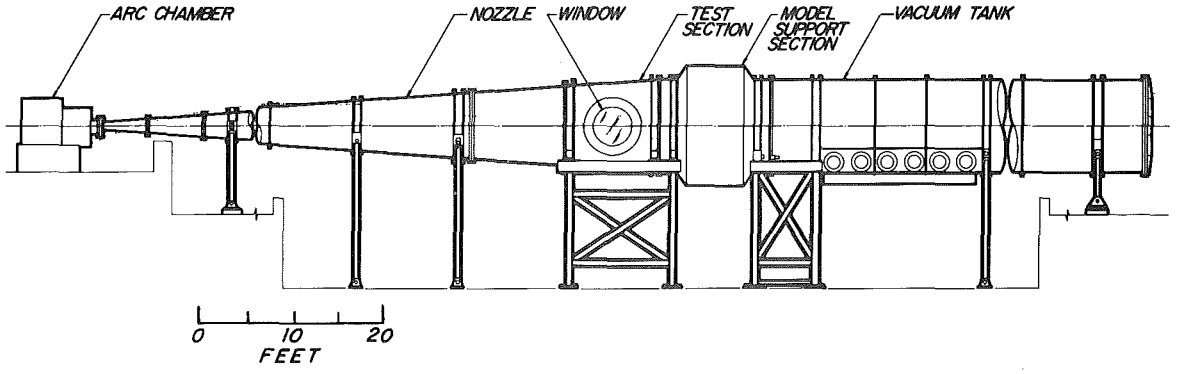

c. 100-Inch Hotshot

Fig. 1 AEDC-VKF Hotshot Tunnels

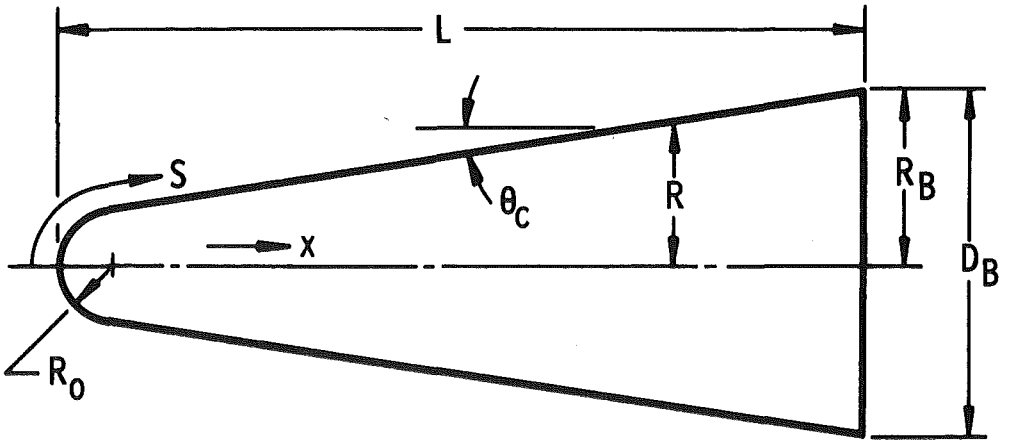

θ_c, deg	ψ	D_B	L	Tunnel
9	0.30	3.00	7.04	AEDC-VKF-Hotshot 2
9	0.30	3.00	7.04	AEDC-VKF-Tunnel F
9	0.30	3.00	7.04	Cal 48 in.
6.34	0.155	3.22	12.49	Cal 48 in.

a. Spherically Blunted Cone

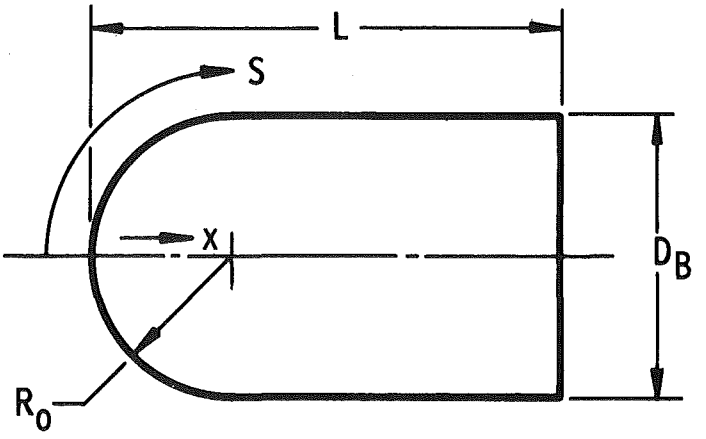

R_0, in.	D_B, in.	L, in.	Tunnel
1.50	3.00	4.50	AEDC-VKF-Hotshot 1
0.50	1.00	2.19	AEDC-VKF-Mach 8

Note: All Dimensions in Inches

b. Hemisphere-Cylinder

Fig. 2 Models

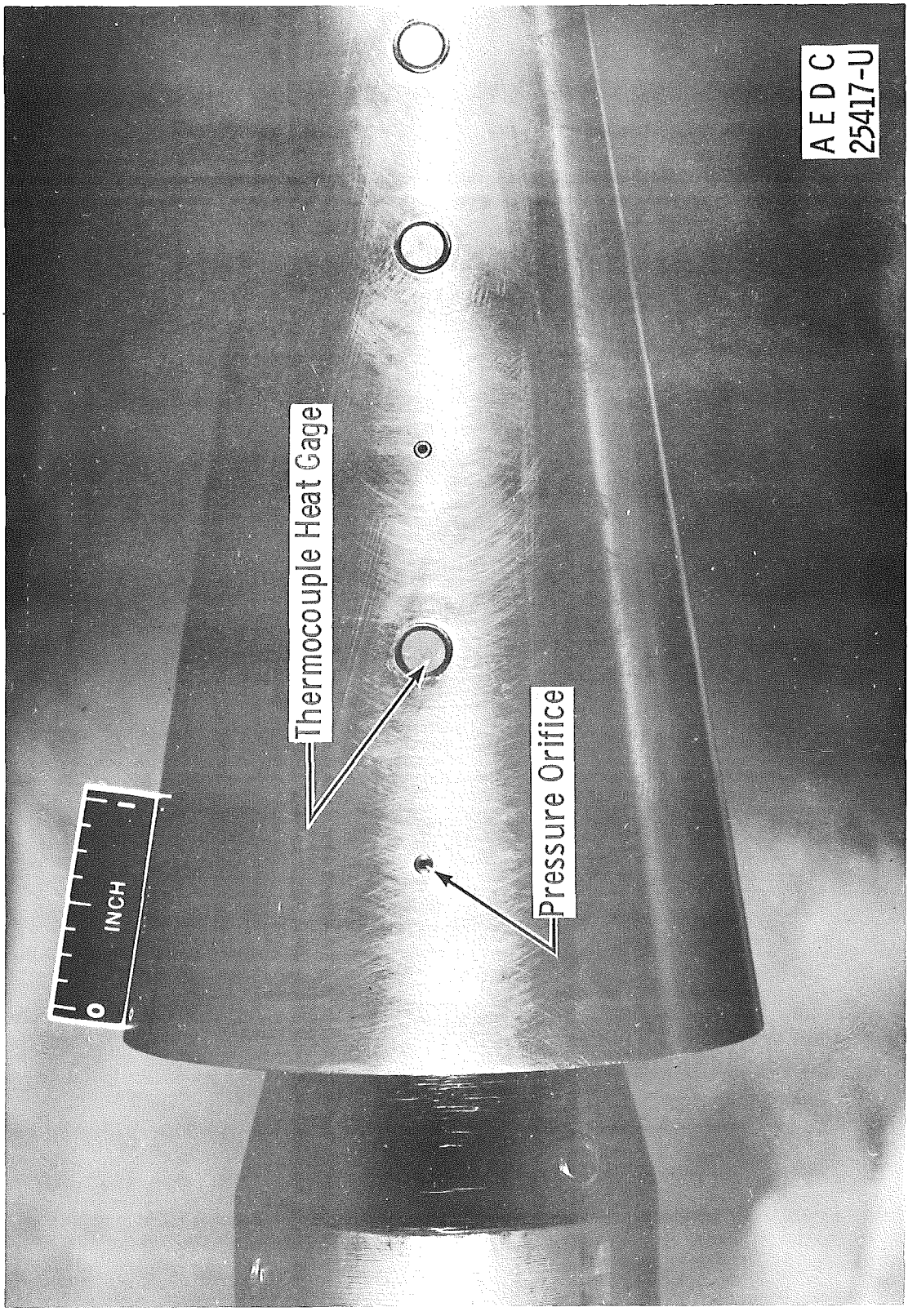

Fig. 3 Spherically Blunted Cone Thermocouple Heat Gage Installation

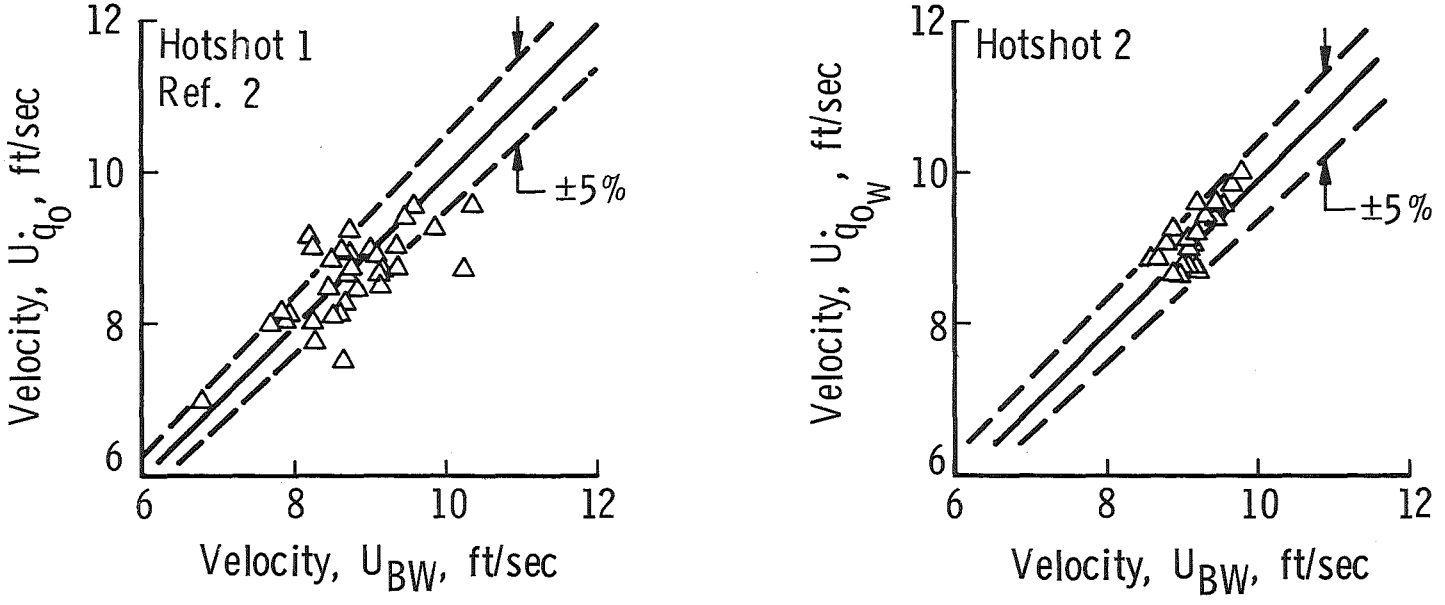

a. Summation of Measured and Calculated Velocities

Fig. 4 Correlation of Flow Velocity Based on Arc-Chamber Measurements and Blast-Wave Velocity Measurements

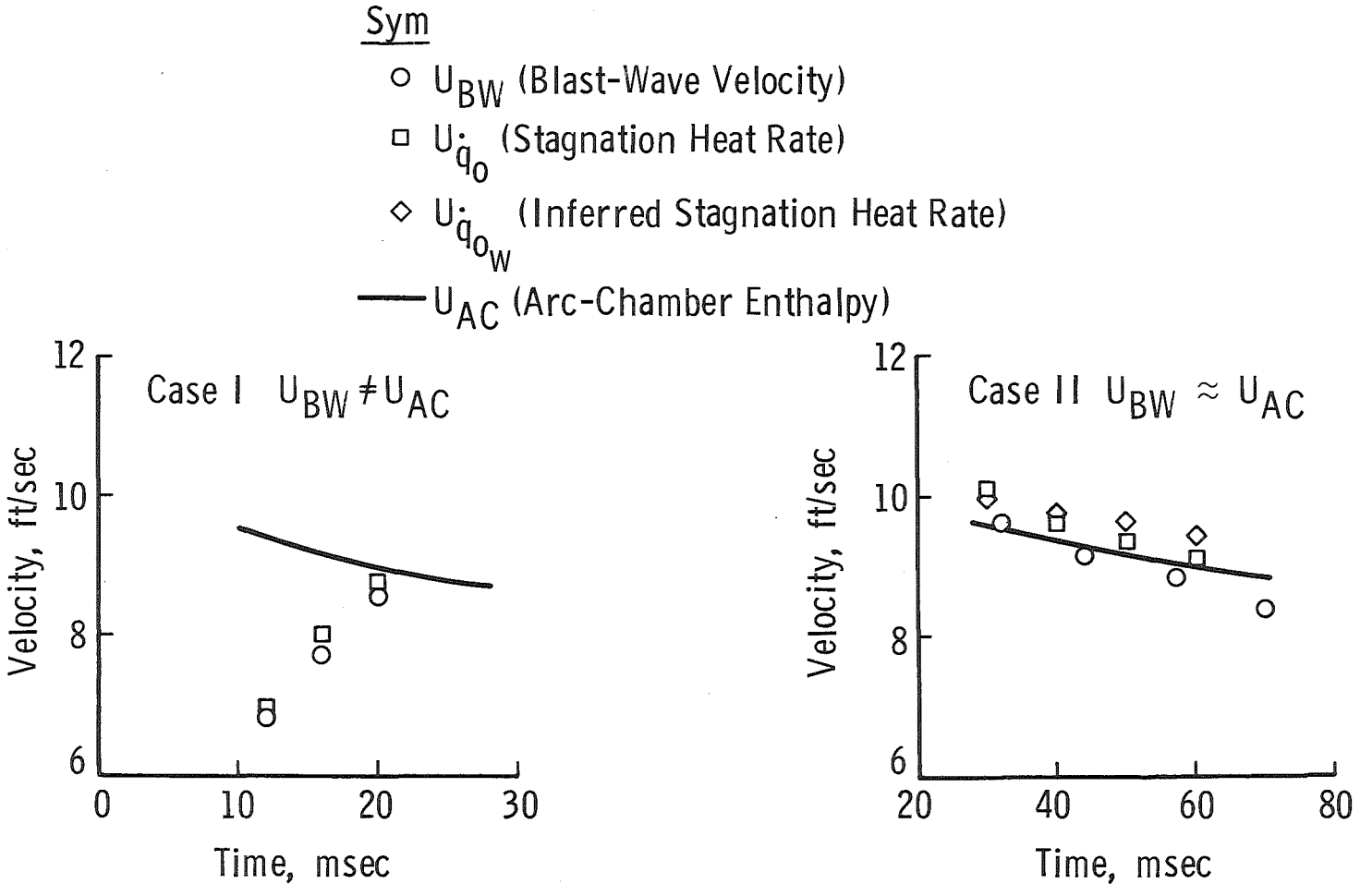

b. Typical Timewise Data

Fig. 4 Concluded

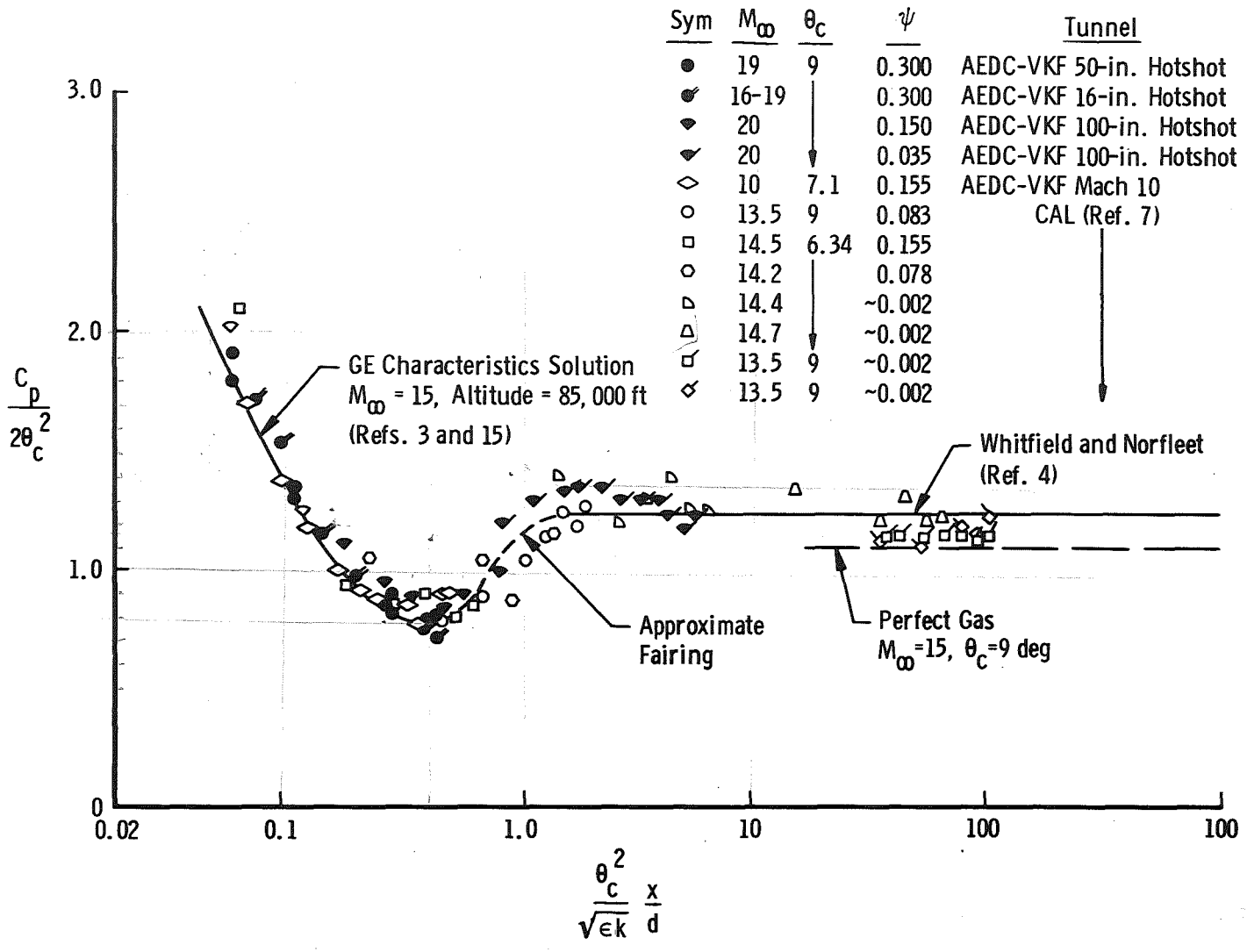

Fig. 5 Correlation of Zero-Lift Cone Pressures, M_∞ = 10 to 20

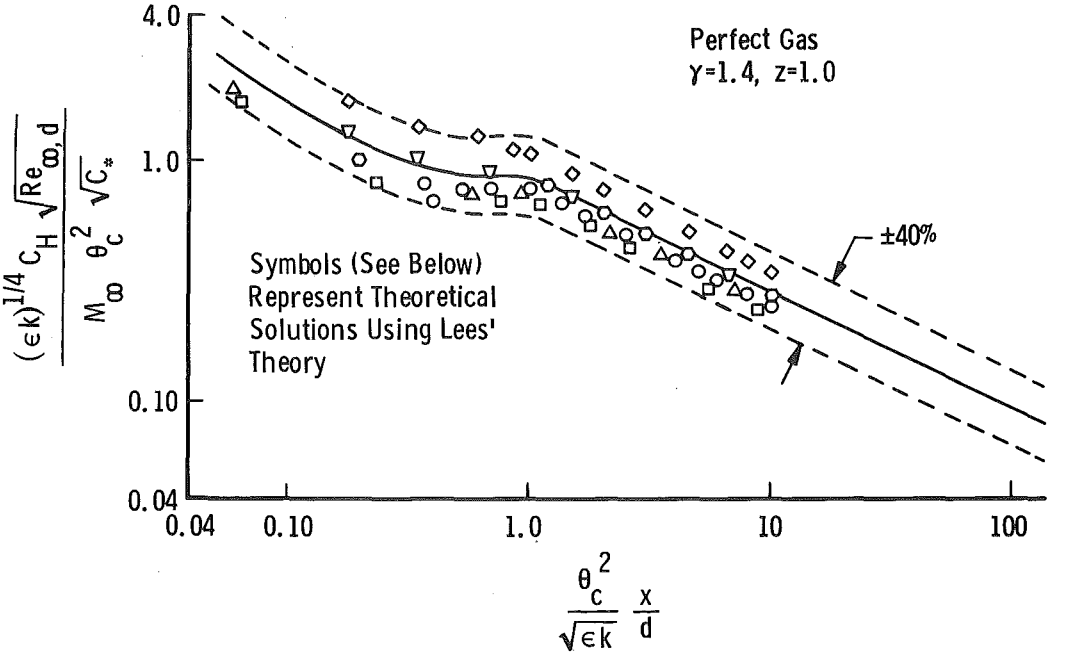

a. Cheng's Correlation Parameter

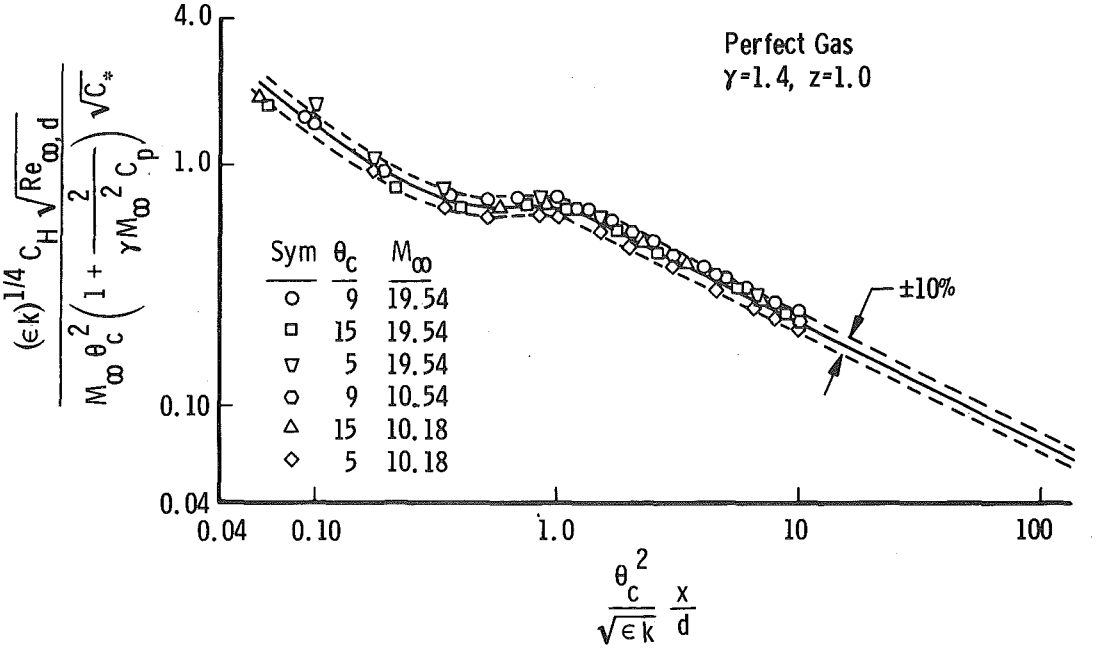

b. A Modified Cheng Correlation Parameter

Fig. 6 Theoretical Heat-Transfer Rates to Blunted Cones Based on Lees' Heat-Transfer Distribution

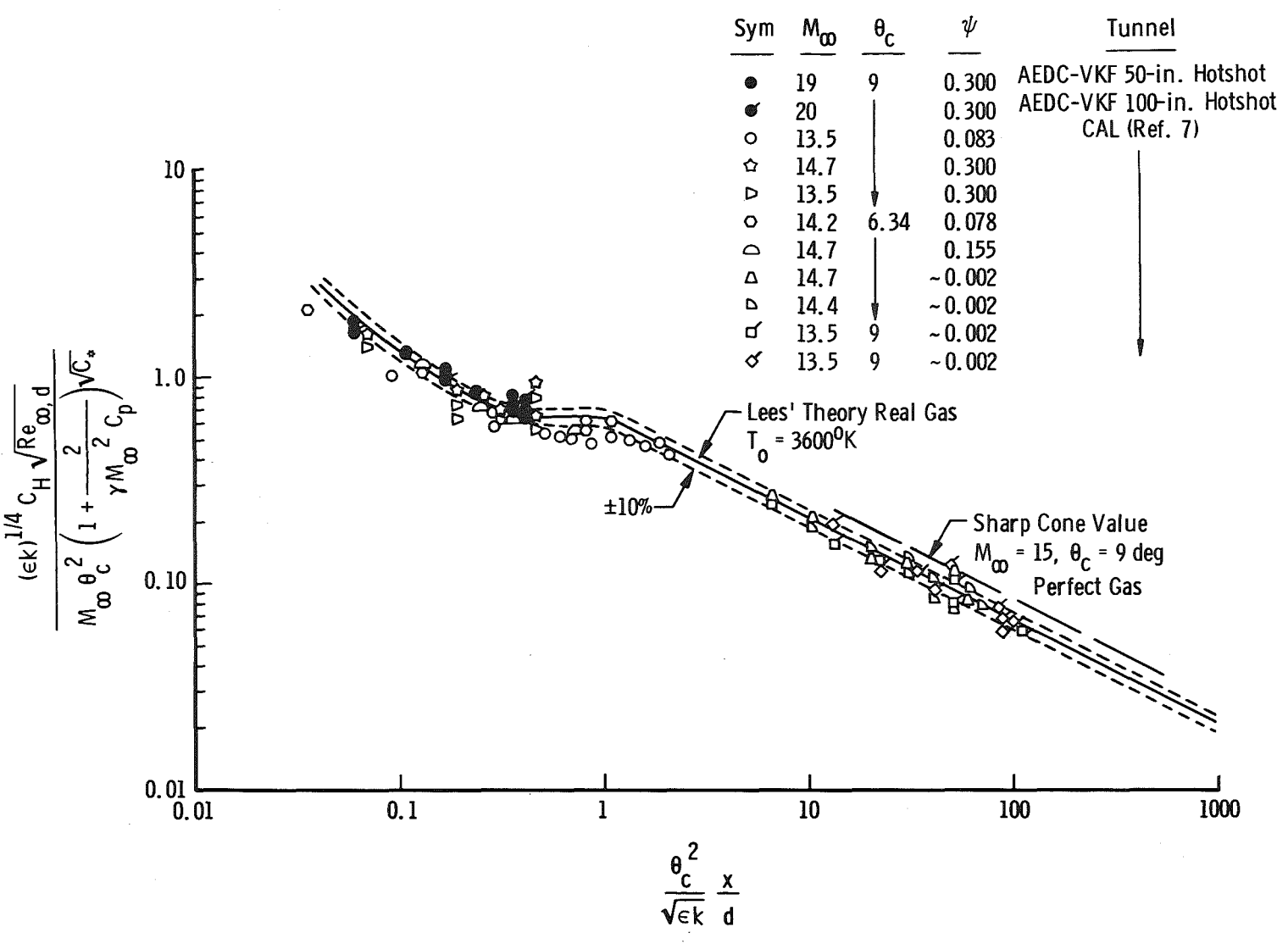

Fig. 7 Comparison of Theoretical and Experimental Heat-Transfer Rates to Spherically Blunted Cones

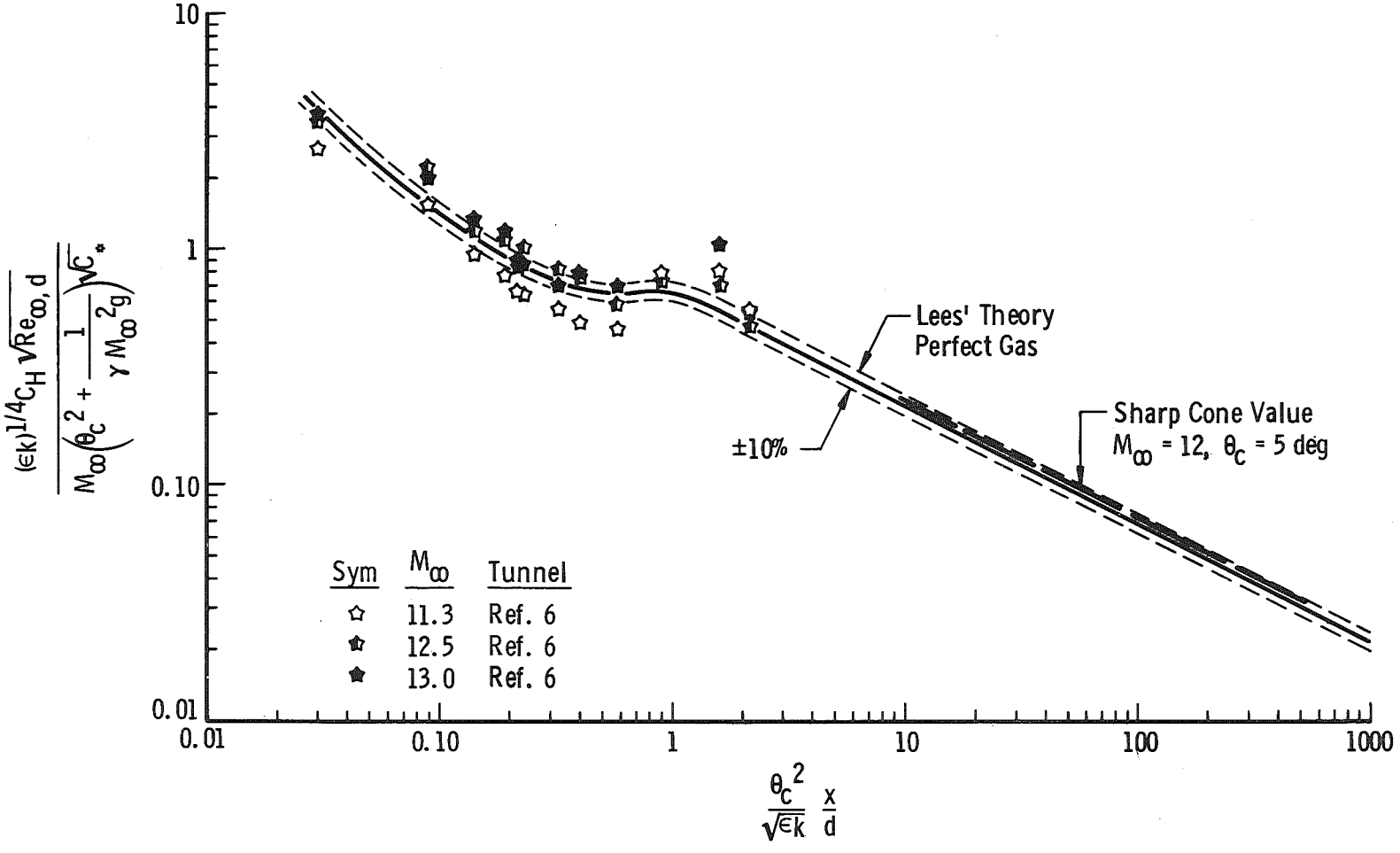

Fig. 8 Comparison of Theoretical and Experimental Heat-Transfer Rates to Flat-Nosed Cones

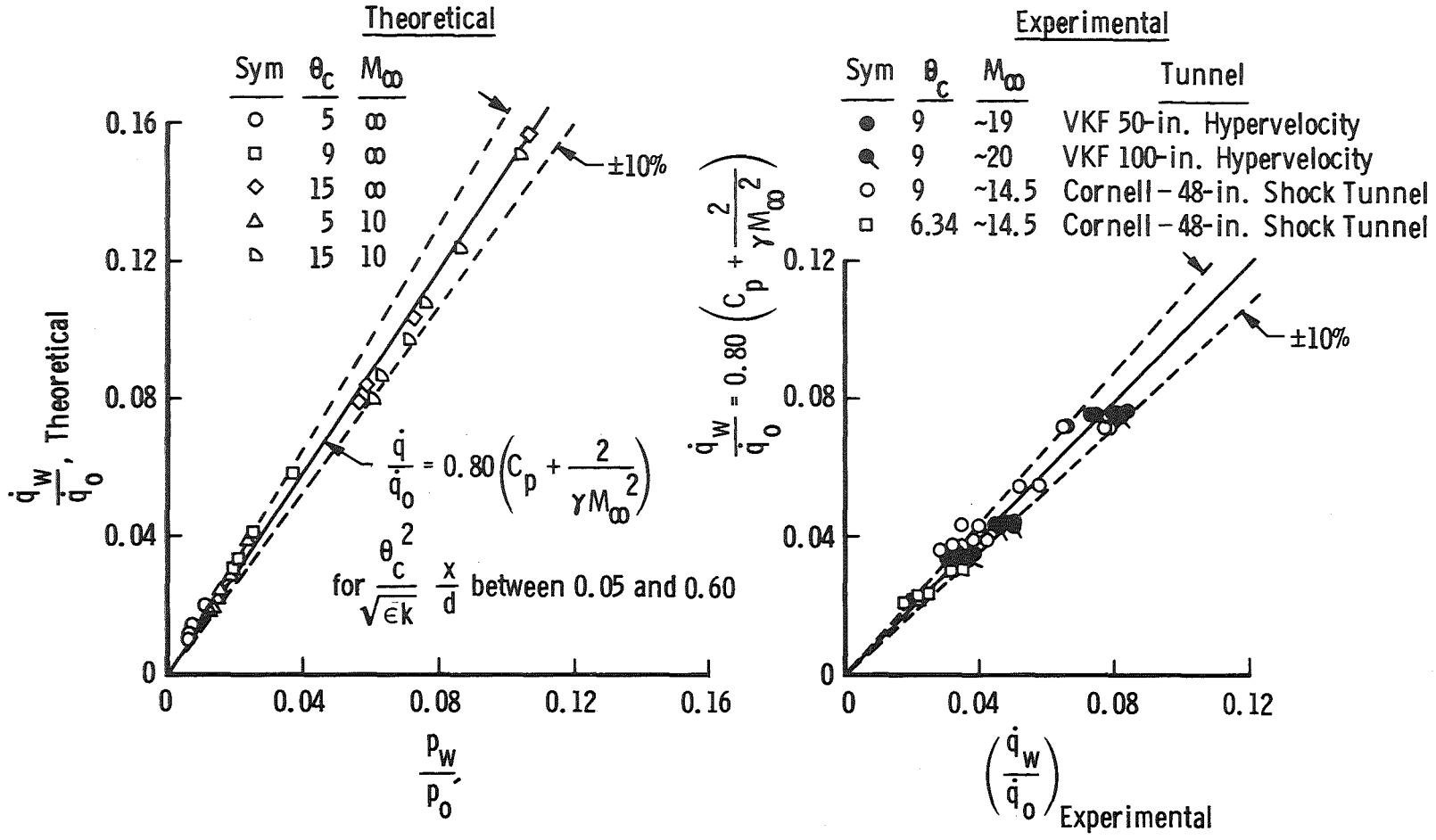

Fig. 9 Correlation of Blunt Cone Heat-Transfer Distribution Data

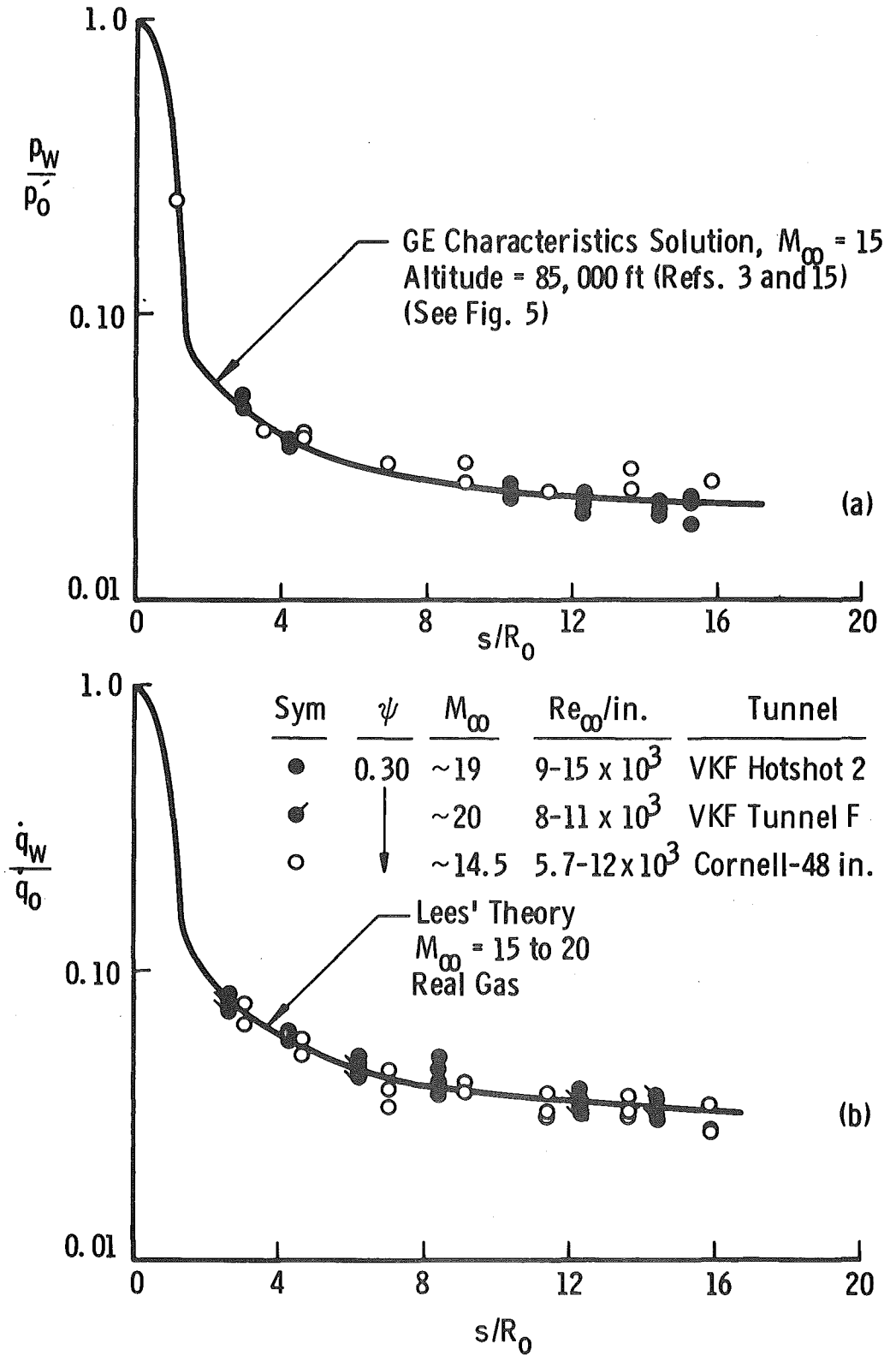

Fig. 10 Heat-Transfer and Pressure Distribution over a 9-deg Half-Angle Blunt Cone

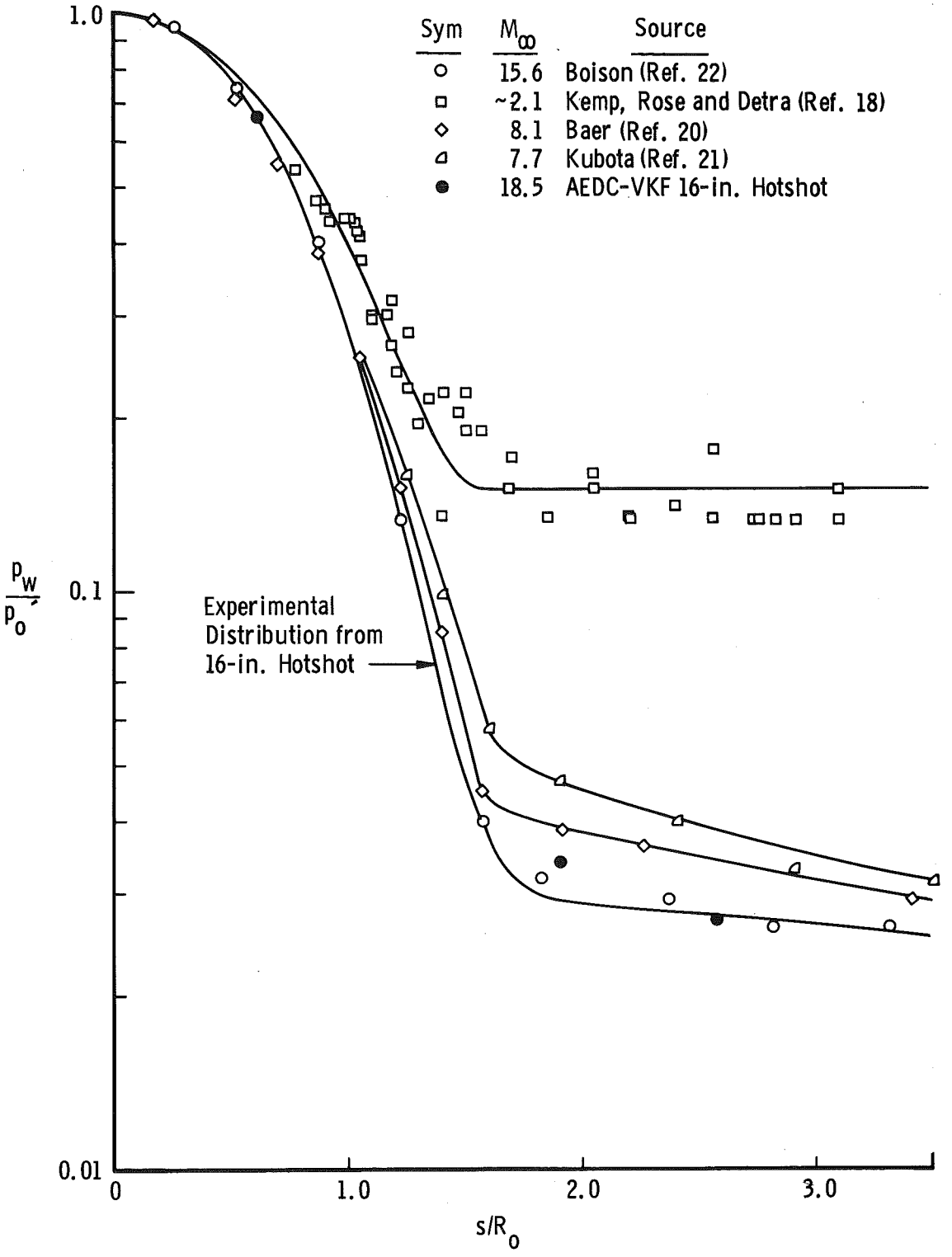

Fig. 11 Pressure Distribution over a Hemisphere-Cylinder

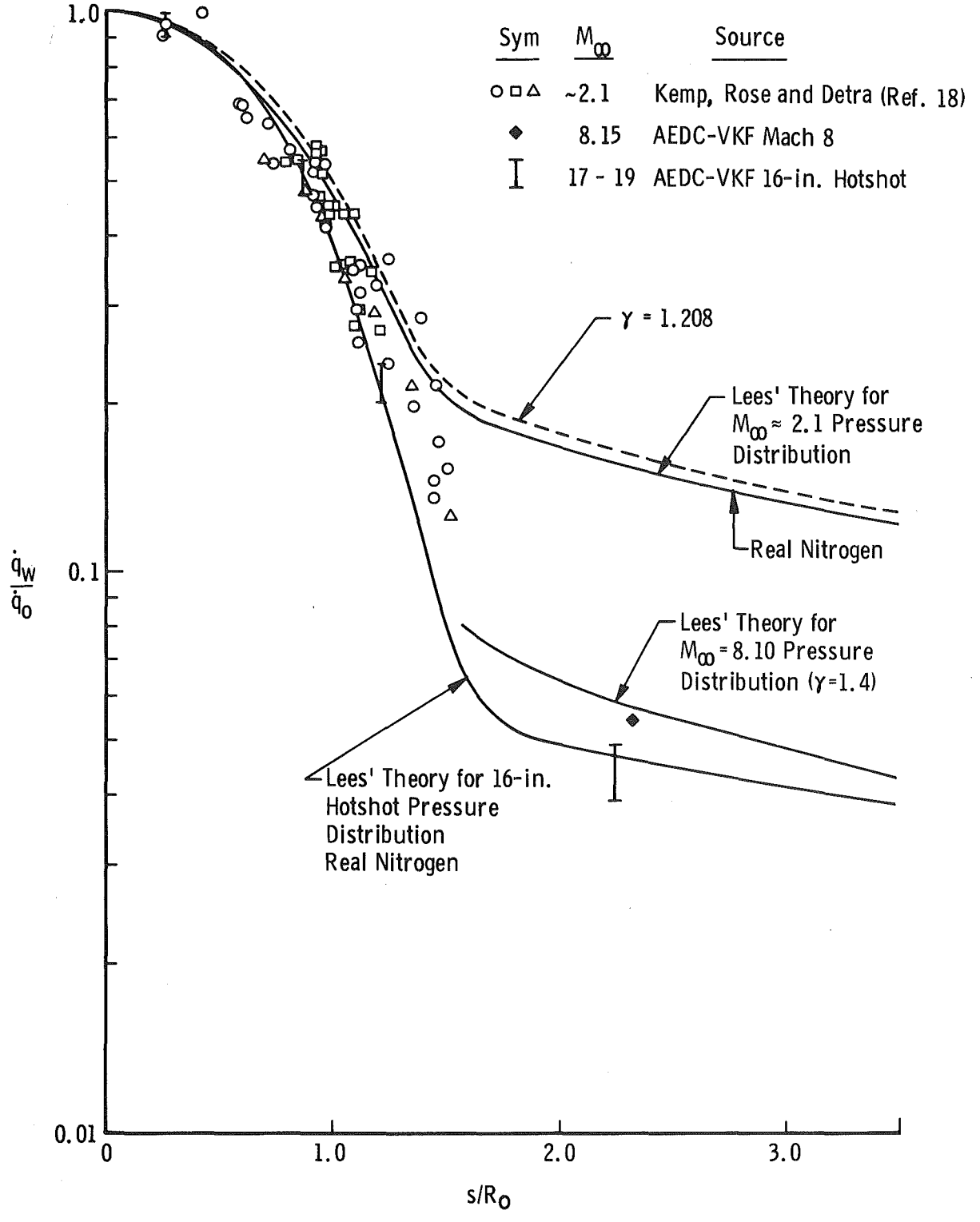

Fig. 12 Heat-Transfer Distribution over a Hemisphere-Cylinder

Arnold Engineering Development Center
Arnold Air Force Station, Tennessee
Rpt. No. AEDC-TDR-63-102. A STUDY OF LAMINAR HEAT TRANSFER TO SPHERICALLY BLUNTED CONES AND HEMISPHERE-CYLINDERS AT HYPERSONIC CONDITIONS. June 1963, 39 p. incl 25 refs., illus.
Unclassified Report

Heat-transfer distribution data obtained in the arc-driven tunnels (hotshot type) of the von Kármán Gas Dynamics Facility, AEDC, are presented. Data were taken on a 9-deg half-angle spherically blunted cone and a hemisphere-cylinder at Mach numbers between 17 and 20 and Reynolds numbers per foot in the free-stream between 100,000 and 800,000. The test data are compared with theory and available shock tube and shock tunnel results. Good agreement between Lees' theory and measured heat-transfer rates demonstrates the capability of the VKF hotshot tunnels to obtain heat-transfer distribution data. The data indicate a strong dependence of the heat-transfer distribution on pressure distribution, Mach number, and cone half-angle. The heat-transfer data are correlated over a wide range of Mach numbers and cone angles. Correlation curves and formulas are presented for the pressure and heat-transfer distribution to spherically blunted cones at hypersonic conditions.

1. Blunt bodies
2. Conical bodies
3. Cylindrical bodies
4. Pressure
5. Heat transfer
6. Hypersonic characteristics
7. Tests
8. Theory
9. Nitrogen

I. AFSC Program Area 806A, Project 8951, Task 895103
II. Contract AF 40(600)-1000
III. ARO, Inc., Arnold AF Sta, Tenn.
IV. B. J. Griffith and C. H. Lewis
V. Available from OTS
VI. In ASTIA Collection

Arnold Engineering Development Center
Arnold Air Force Station, Tennessee
Rpt. No. AEDC-TDR-63-102. A STUDY OF LAMINAR HEAT TRANSFER TO SPHERICALLY BLUNTED CONES AND HEMISPHERE-CYLINDERS AT HYPERSONIC CONDITIONS. June 1963, 39 p. incl 25 refs., illus.
Unclassified Report

Heat-transfer distribution data obtained in the arc-driven tunnels (hotshot type) of the von Kármán Gas Dynamics Facility, AEDC, are presented. Data were taken on a 9-deg half-angle spherically blunted cone and a hemisphere-cylinder at Mach numbers between 17 and 20 and Reynolds numbers per foot in the free-stream between 100,000 and 800,000. The test data are compared with theory and available shock tube and shock tunnel results. Good agreement between Lees' theory and measured heat-transfer rates demonstrates the capability of the VKF hotshot tunnels to obtain heat-transfer distribution data. The data indicate a strong dependence of the heat-transfer distribution on pressure distribution, Mach number, and cone half-angle. The heat-transfer data are correlated over a wide range of Mach numbers and cone angles. Correlation curves and formulas are presented for the pressure and heat-transfer distribution to spherically blunted cones at hypersonic conditions.

1. Blunt bodies
2. Conical bodies
3. Cylindrical bodies
4. Pressure
5. Heat transfer
6. Hypersonic characteristics
7. Tests
8. Theory
9. Nitrogen

I. AFSC Program Area 806A, Project 8951, Task 895103
II. Contract AF 40(600)-1000
III. ARO, Inc., Arnold AF Sta, Tenn.
IV. B. J. Griffith and C. H. Lewis
V. Available from OTS
VI. In ASTIA Collection

Arnold Engineering Development Center
Arnold Air Force Station, Tennessee
Rpt. No. AEDC-TDR-63-102. A STUDY OF LAMINAR HEAT TRANSFER TO SPHERICALLY BLUNTED CONES AND HEMISPHERE-CYLINDERS AT HYPERSONIC CONDITIONS. June 1963, 39 p. incl 25 refs., illus.
Unclassified Report

Heat-transfer distribution data obtained in the arc-driven tunnels (hotshot type) of the von Kármán Gas Dynamics Facility, AEDC, are presented. Data were taken on a 9-deg half-angle spherically blunted cone and a hemisphere-cylinder at Mach numbers between 17 and 20 and Reynolds numbers per foot in the free-stream between 100,000 and 800,000. The test data are compared with theory and available shock tube and shock tunnel results. Good agreement between Lees' theory and measured heat-transfer rates demonstrates the capability of the VKF hotshot tunnels to obtain heat-transfer distribution data. The data indicate a strong dependence of the heat-transfer distribution on pressure distribution, Mach number, and cone half-angle. The heat-transfer data are correlated over a wide range of Mach numbers and cone angles. Correlation curves and formulas are presented for the pressure and heat-transfer distribution to spherically blunted cones at hypersonic conditions.

1. Blunt bodies
2. Conical bodies
3. Cylindrical bodies
4. Pressure
5. Heat transfer
6. Hypersonic characteristics
7. Tests
8. Theory
9. Nitrogen

I. AFSC Program Area 806A, Project 8951, Task 895103
II. Contract AF 40(600)-1000
III. ARO, Inc., Arnold AF Sta, Tenn.
IV. B. J. Griffith and C. H. Lewis
V. Available from OTS
VI. In ASTIA Collection

Arnold Engineering Development Center
Arnold Air Force Station, Tennessee
Rpt. No. AEDC-TDR-63-102. A STUDY OF LAMINAR HEAT TRANSFER TO SPHERICALLY BLUNTED CONES AND HEMISPHERE-CYLINDERS AT HYPERSONIC CONDITIONS. June 1963, 39 p. incl 25 refs., illus.
Unclassified Report

Heat-transfer distribution data obtained in the arc-driven tunnels (hotshot type) of the von Kármán Gas Dynamics Facility, AEDC, are presented. Data were taken on a 9-deg half-angle spherically blunted cone and a hemisphere-cylinder at Mach numbers between 17 and 20 and Reynolds numbers per foot in the free-stream between 100,000 and 800,000. The test data are compared with theory and available shock tube and shock tunnel results. Good agreement between Lees' theory and measured heat-transfer rates demonstrates the capability of the VKF hotshot tunnels to obtain heat-transfer distribution data. The data indicate a strong dependence of the heat-transfer distribution on pressure distribution, Mach number, and cone half-angle. The heat-transfer data are correlated over a wide range of Mach numbers and cone angles. Correlation curves and formulas are presented for the pressure and heat-transfer distribution to spherically blunted cones at hypersonic conditions.

1. Blunt bodies
2. Conical bodies
3. Cylindrical bodies
4. Pressure
5. Heat transfer
6. Hypersonic characteristics
7. Tests
8. Theory
9. Nitrogen

I. AFSC Program Area 806A, Project 8951, Task 895103
II. Contract AF 40(600)-1000
III. ARO, Inc., Arnold AF Sta, Tenn.
IV. B. J. Griffith and C. H. Lewis
V. Available from OTS
VI. In ASTIA Collection